Journal of
Experimental
Botany
www.jxb.oxfordjournals.org

RESEARCH PAPER

Characterization of leaf apoplastic peroxidases and metabolites in *Vigna unguiculata* in response to toxic manganese supply and silicon

Hendrik Führs[1], Stefanie Götze[1], André Specht[1], Alexander Erban[2], Sébastien Gallien[3], Dimitri Heintz[4], Alain Van Dorsselaer[3], Joachim Kopka[2], Hans-Peter Braun[5] and Walter J. Horst[1],*

[1] Institute of Plant Nutrition, Faculty of Natural Sciences, Leibniz University Hannover, Herrenhäuser Str. 2, D-30419 Hannover, Germany

[2] Max Planck Institute of Molecular Plant Physiology, Am Mühlenberg 1, D-14476 Potsdam-Golm, Germany

[3] Laboratoire de Spectrométrie de Masse Bio-Organique, IPHC-DSA, ULP, CNRS, UMR7178 ; 25 rue Becquerel, F-67087 Strasbourg, France

[4] Institut de Biologie Moléculaire des Plantes (IBMP) CNRS-UPR2357,ULP, F-67083 Strasbourg, France

[5] Institute of Plant Genetics, Faculty of Natural Sciences, Leibniz University Hannover, Herrenhäuser Str. 2, D-30419 Hannover, Germany

Abstract

Previous work suggested that the apoplastic phenol composition and its interaction with apoplastic class III peroxidases (PODs) are decisive in the development or avoidance of manganese (Mn) toxicity in cowpea (*Vigna unguiculata* L.). This study characterizes apoplastic PODs with particular emphasis on the activities of specific isoenzymes and their modulation by phenols in the Mn-sensitive cowpea cultivar TVu 91 as affected by Mn and silicon (Si) supply. Si reduced Mn-induced toxicity symptoms without affecting the Mn uptake. Blue Native-PAGE combined with Nano-LC-MS/MS allowed identification of a range of POD isoenzymes in the apoplastic washing fluid (AWF). In Si-treated plants Mn-mediated induction of POD activity was delayed. Four POD isoenzymes eluted from the BN gels catalysed both H_2O_2-consuming and H_2O_2-producing activity with pH optima at 6.5 and 5.5, respectively. Four phenols enhanced NADH-*per*oxidase activity of these isoenzymes in the presence of Mn^{2+} (*p*-coumaric$=$vanillic$>>$benzoic$>$ferulic acid). *p*-Coumaric acid-enhanced NADH-*per*oxidase activity was inhibited by ferulic acid (50%) and five other phenols (50–90%). An independent component analysis (ICA) of the total and apoplastic GC-MS-based metabolome profile showed that Mn, Si supply, and the AWF fraction (AWF_{H_2O}, AWF_{NaCl}) significantly changed the metabolite composition. Extracting non-polar metabolites from the AWF allowed the identification of phenols. Predominantly NADH-*per*oxidase activity-inhibiting ferulic acid appeared to be down-regulated in Mn-sensitive (+Mn, –Si) and up-regulated in Mn-tolerant (+Si) leaf tissue. The results presented here support the previously hypothesized role of apoplastic NADH-*per*oxidase and its activity-modulating phenols in Mn toxicity and Si-enhanced Mn tolerance.

Key words: BN-PAGE, cowpea, leaf apoplast, metabolome, manganese toxicity, phenolics, proteome.

Introduction

Manganese (Mn) in plants is an essential micronutrient (Marschner, 1995). However, at supra-optimum supply Mn readily becomes toxic to plants. Mn toxicity in crops is a widely distributed plant disorder mainly on acidic and insufficiently drained soils with low redox potentials thus leading to high amounts of plant-available Mn (Horst, 1988).

In cowpea, Mn-resistant cultivars do not differ in Mn accumulation from Mn-sensitive cultivars (Horst, 1980;

Führs *et al.*, 2008). Therefore, in this species Mn resistance is regarded as Mn tolerance (Horst, 1983). Typical Mn stress-induced toxicity symptoms in cowpea develop primarily on older leafs as distinct brown spots located in the leaf apoplast of the epidermis starting at the leaf base, then spreading to the tip, followed by chlorosis, and, finally, leaf shedding (Horst and Marschner, 1978b; Horst, 1982).

The brown spots consist of oxidized Mn and oxidized phenolic compounds (Wissemeier and Horst, 1992). Hence, the oxidaton of Mn^{2+} and phenols mediated by apoplastic PODs was proposed to be a key reaction leading to Mn toxicity (Fecht-Christoffers *et al.*, 2006). Class III apoplastic PODs (EC 1.11.17) belong to multigenic families (Passardi *et al.*, 2004) with various functions in plant growth (for more information see Passardi *et al.*, 2005). PODs are polyfunctional enzymes that undergo two reaction cycles: the peroxidase–oxidase cycle (with NADH as substrate also called NADH-*per*oxidases) resulting in H_2O_2 production (Halliwell, 1978) and the peroxidase cycle (with guaiacol as phenol substrate also called guaiacol-peroxidase) leading to H_2O_2 consumption (Fecht-Christoffers *et al.*, 2003a, b). H_2O_2-producing POD activity was intensively studied with respect to numerous exogenous factors like ambient pH (Bolwell *et al.*, 1995, 2001), phenol composition (Halliwell, 1978; Fecht-Christoffers *et al.*, 2006), and Mn^{2+} concentration *in vivo* (Yamazaki and Piette, 1963; Halliwell, 1978)

Fecht-Christoffers *et al.* (2006, 2007) investigated H_2O_2-producing activity of apoplastic peroxidases of cowpea *in vitro* and found that not only Mn^{2+} but also phenols are required to induce NADH-*per*oxidase activity. Increasing Mn concentrations in the leaf tissue and the AWF affected the total apoplastic phenol concentration and composition. Crosswise combining of AWF metabolites with AWF proteins from cultivars differing in Mn tolerance revealed a significant effect on NADH-*per*oxidase activity. They concluded that the apoplastic phenol composition and its interaction with PODs are decisive in the development or avoidance of Mn toxicity.

Silicon is a beneficial element for most plants (Epstein, 1999), and alleviates heavy metal toxicities, for example, aluminium and Mn toxicity. The alleviative effect of Si on Mn toxicity was described for common bean and cowpea (Horst and Marschner, 1978a; Iwasaki *et al.*, 2002a, b), cucumber (Rogalla and Römheld, 2002; Shi *et al.*, 2005), and pumpkin (Iwasaki and Matsumura, 1999). For cowpea, Horst and Marschner (1978a) found that leaf Mn was more evenly distributed in Si-treated cowpea plants. Horst *et al.* (1999) demonstrated a reduction in apoplastic Mn concentrations due to Si supply and concluded that Si changes apoplastic Mn-binding properties, even though this could only partly explain Si-mediated alleviation of Mn toxicity (Iwasaki *et al.*, 2002b). It was found that toxicity symptoms and guaiacol-peroxidase activities were more closely related to apoplastic Si concentrations than to apoplastic Mn concentrations, indicating a more direct involvement of Si nutrition in detoxification of apoplastic Mn.

The work presented here specifically addressed the hypothesis that the activities of specific apoplastic peroxidases and their modulation by metabolites are decisive for Mn toxicity and Si-induced enhanced Mn tolerance in the Mn-sensitive cowpea cultivar TVu 91.

Materials and methods

Plant material

Cowpea [*Vigna unguiculata* (L.) Walp., cv. TVu 91] was grown hydroponically in a growth chamber under controlled environmental conditions at 30/27 °C day/night temperatures, 75±5% relative humidity, and a photon flux density of 150 μmol m^{-1} s^{-1} photosynthetic active radiation (*PAR*) at mid-plant height during a 16 h photoperiod. After germination in 1 mM $CaSO_4$ for 7 d, seedlings were transferred to a constantly aerated nutrient solution with four plants in one 5.0 l pot. The composition of the nutrient solution was (μM): $Ca(NO_3)_2$ 1000, KH_2PO_4 100, K_2SO_4 375, $MgSO_4$ 325, FeEDDHA 20, NaCl 10, H_3BO_3 8, $MnSO_4$ 0.2, $CuSO_4$ 0.2, $ZnSO_4$ 0.2, Na_2MoO_4 0.05. Silicon-treated plants (+Si) received Si in form of Aerosil (Horst and Marschner, 1978a; chemically clean silicic acid, solubility in water: 0.6–0.75 mg l^{-1} or 20–26.5 μM). After preculture for 14 d, the Mn concentration in the nutrient solution was increased from 0.2 μM (–Mn) to 50 μM (+Mn) for 4 d or 6 d. The nutrient solution was changed two to three times per week to avoid nutrient deficiencies.

Extraction of water-soluble and ionically bound apoplastic proteins and metabolites

Apoplastic washing fluid (AWF) was extracted by a vacuum infiltration/centrifugation technique according to Fecht-Christoffers *et al.* (2003a, b). Leaves were infiltrated with chilled dH_2O by reducing the pressure to –35 hPa followed by a slow relaxation. AWF_{H_2O} was recovered by centrifugation at 1324 *g* for 5 min at 4 °C. Afterwards, the same leaves were infiltrated with chilled 0.5 M NaCl solution and AWF_{NaCl} was recovered as described above. Malate dehydrogenase (MDH) activity in both AWF fractions showed a cytoplasmic contamination of less than 1% (data not shown). Until further analysis the AWF was stored at –80 °C.

Quantification of toxicity symptoms

For the quantification of Mn toxicity symptoms, the density of brown spots was counted on a 1.54 cm^2 area at the base and tip on the upper side of the second oldest middle trifoliate leaf and calculated on 1 cm^2 base.

Manganese analysis

Manganese in the bulk-leaf tissue was determined in the second oldest middle trifoliate leaf after dry ashing at 480 °C for 8 h, dissolving the ash in 6 M HCl with 1.5% (w/v) hydroxylammonium chloride, and then diluting (1:10 v/v) with double demineralized water. Apoplastic Mn concentrations were measured in 1:10 dilutions of the AWF. Both

measurements were carried out by optical inductively-coupled plasma-emission spectroscopy (Spectro Analytical Instruments GmbH, Kleve, Germany).

Silicon analysis

Monomeric Si concentration in the AWF was determined according to Iwasaki *et al.* (2002*a*, *b*). AWF and a standard solution (0–100 µg Si ml^{-1} AWF) were mixed with 250 µl of staining solution (1:1 mix of 0.08 M H_2SO_4 and 20 g l^{-1} $(NH_4)_6Mo_7O_{24}.4H_2O$). After 30 min of incubation 250 µl of freshly prepared ascorbic acid (0.1 g 25 ml^{-1}) and 250 µl tartaric acid (0.85 g 25 ml^{-1}) were added. Samples were measured at λ=811 nm in a Microplate-Reader (µQuant, BioTek Instruments, Germany).

Determination of the protein concentration in the AWF and AWF concentrates

The protein concentration in the AWF for the calculation of specific enzyme activities was determined according to Bradford (1976). The protein concentration of AWF concentrates was measured for 1D BN-PAGE using the 2-D Quant Kit© (GE Healthcare, USA) according to the manufacturer's instructions.

Determination of specific peroxidase activities in the AWF

For the measurement of H_2O_2-consuming guaiacol-peroxidase activities in the AWF, the oxidation of the substrate guaiacol was determined spectrophotometrically at λ=470 nm (UVIKON 943, BioTek Instruments GmbH, Neufahrn, Germany). Samples were mixed with guaiacol solution (20 mM guaiacol in 10 mM Na_2HPO_4 buffer, pH 6) and 0.03% (v/v) H_2O_2. For calculation of enzyme activities the molar extinction coefficient 26.6 l (mmol cm)$^{-1}$ was used.

For the measurement of the H_2O_2-producing NADH-*per*oxidase activity in the AWF, samples were mixed with $MnCl_2$ (16 mM), *p*-coumaric acid (1.6 mM) and NADH (0.22 mM). The NADH oxidation-dependent decline in absorption at λ=340 nm was determined. For calculation of enzyme activities the molar extinction coefficient 1.13 l (mmol cm)$^{-1}$ was used.

1D BN-PAGE of apoplastic proteins and POD activity staining

For protein separation by electrophoresis under native conditions, the proteins of the AWF were concentrated at 4 °C by using centrifugal concentrators with a molecular mass cut-off at 5 kDa (Vivaspin 6, Vivascience, Hannover, Germany). Running conditions were used according to the manufacturer's instructions.

Proteins were separated via BN-PAGE according to Jänsch *et al.* (1996). Protein samples were combined with Coomassie Blue solution [5% (w/v) Serve Blue G and 750 mM aminocaproic acid] and 10% (v/v) glycerol (100%). Samples were loaded onto a native acrylamide gel with a 4% (w/v) stacking gel and a 12% to 20% (w/v) gradient separation gel. Electrophoresis was carried out at 100 V and 6–8 mA for 45 min followed by 13 h at 15 mA (max. 500 V).

NADH-*per*oxidase activity in the gel was determined by NBT staining to detect O_2^- radicals or by DAB staining (data not shown) to detect H_2O_2. The staining solution finally consisted of 16 mM $MnCl_2$, 1.6 mM *p*-coumaric acid, 0.22 mM NADH, and 2.5 mg ml^{-1} NBT in order to detect O_2^- radicals, that are proposed to be produced during the NADH-*per*oxidase activity of PODs (Halliwell, 1978) because a direct detection of H_2O_2 by DAB staining was difficult due to the high gel background caused by Coomassie. Gels were stained for 30 min at room temperature. The gels were afterwards soaked in 20 mM guaiacol (in 10 mM Na_2HPO_4) and 0.03% (v/v) H_2O_2 for 3 min to dectect guaiacol-peroxidase activity.

For preparative BN-PAGE guaiacol-peroxidase staining was carried out only for a few seconds in order to reduce enzyme damage by product–enzyme interaction.

Electroelution of specific POD isoenzymes for further physiological characterization

Four POD isoenzymes (P1, P3, P5, and P6 in Fig. 3C) were chosen for electroelution from BN gels that was carried out according to Wehrhahn and Braun (2002). POD isoenzymes were cut from the gel and incubated for 30 min in cathodic buffer [50 mM Tricine, 15 mM BIS-TRIS, 0.1 % (w/v) Coomassie 250 G, pH 7 adjusted at 4 °C] and transferred into the chambers of an electroeluter (CBS SCIENTIFIC, Del Mar, USA). The gel pieces containing the POD isoenzymes were filled into the electroeluter containing elution buffer (25 mM Tricine, 7.5 mM BIS-TRIS, pH 7.0 adjusted at 4 °C). Electroelution was carried out for 5 h and 4 °C at 350 V and 6–10 mA, using dialysis membranes (Medicell, Kleinfeld) with a MWCO of 12–14 kDa under constant buffer circulation (Econopump, Bio-Rad Laboratories, CA, USA). Until further characterization, eluates were stored at –80 °C.

Determination of the pH optimum of the guaiacol-peroxidase and NADH-*per*oxidase activity of POD isoenzymes

For guaiacol-peroxidase measurements, 6 µl eluate was mixed with guaiacol (20 mM) in 0.1 M succinate buffer with the pH values 5, 5.5, 6, 6.5, and 7. The reaction was started by adding 0.3% (v/v) H_2O_2. The increase in absorption was measured at λ=470 nm using a Microplate Reader. For calculation of enzyme activities the molar extinction coefficient 26.6 l (mmol cm)$^{-1}$ was used.

NADH-*per*oxidase activity measurements were made by combining $MnCl_2$, *p*-coumaric acid, and NADH in final concentrations of 16 mM, 1.6 mM, and 0.66 mM, respectively, with 7.5 µl protein eluate in 0.1 M succinate buffer (as described above). The decline in absorption was determined using a Microplate Reader at λ=340 nm. For

calculation of enzyme activities the molar extinction co-efficient 1.13 l (mmol cm)$^{-1}$ was used.

Determination of cofactor specificity for NADH-peroxidase activity of POD isoenzymes

The same experimental set-up as for the determination of the pH optimum was followed using succinate buffer (pH 5.5). *p*-Coumaric acid was substituted by benzoic acid, caffeic acid, chlorogenic acid, ferulic acid, gallic acid, protocatechuic acid, syringic acid, vanillic acid, and *p*-hydroxybenzoic acid in four different concentrations (1.66 mM, 0.166 mM, 0.0166 mM, and 0.00166 mM) in the measuring solution. In order to simplify this report, benzoic acid as an aromatic carboxylic acid is termed as a phenolic acid, too. For each phenol concentration specific extinction coefficients were determined and used for enzyme activity calculation (see Supplementary Table S1 at *JXB* online).

Determination of changes in NADH-peroxidase activity of POD isoenzymes as affected by combining different phenols with p-coumaric acid

To detect the effects of different phenols on *p*-coumaric acid-stimulated NADH-*per*oxidase activity of different iso-enzymes separated by BN-PAGE 0.166 mM *p*-coumaric acid was combined with benzoic acid, caffeic acid, chloro-genic acid, ferulic acid, gallic acid, protocatechuic acid, syringic acid, vanillic acid, and *p*-hydroxybenzoic acid each at a concentration of 0.0166 mM. All other factors were kept as described for the measurement of cofactor specificity. Activity was expressed as a percentage of *p*-coumaric acid induced NADH-*per*oxidase activitiy. For each phenol concentration, specific extinction coefficients were deter-mined and used for enzyme activity calculation (see Supplementary Table S1 at *JXB* online).

Mass spectrometric protein analysis and data interpretation

Marked BN-PAGE bands stained for guaiacol-peroxidase activity were cut and dried under vacuum. In-gel digestion was performed with an automated protein digestion system, MassPREP Station (Micromass, Manchester, UK). The gel slices were washed three times in a mixture containing 25 mM NH$_4$HCO$_3$:acetonitrile (1:1, v/v). The cysteine residues were reduced by 50 μl of 10 mM dithiothreitol at 57 °C and alkylated by 50 μl of 55 mM iodacetamide. After de-hydration with acetonitrile, the proteins were cleaved in the gel with 40 μl of 12.5 ng μl^{-1} of modified porcine trypsin (Promega, Madison, WI, USA) in 25 mM NH$_4$HCO$_3$ at room temperature for 14 h. The resulting tryptic peptides were extracted with 60% acetonitrile in 0.5% formic acid, followed by a second extraction with 100% (v/v) acetoni-trile.

Nano-LC-MS/MS analysis of the resulting tryptic pep-tides was performed using using an Agilent 1100 series HPLC-Chip/MS system (Agilent Technologies, Palo Alto, USA) coupled to an HCT Ultra ion trap (Bruker Daltonics,

Bremen, Germany). Chromatographic separations were conducted on a chip containing a Zorbax 300SB-C18 (75 μm inner diameter×150 mm) column and a Zorbax 300SB-C18 (40 nl) enrichment column (Agilent Technologies).

HCT Ultra ion trap was externally calibrated with standard compounds. The general mass spectrometric parameters were as follows: capillary voltage, –1750 V; dry gas, 3.0 l min^{-1}; dry temperature, 300 °C. The system was operated with automatic switching between MS and MS/MS modes. The MS scanning was performed in the standard-enhanced resolution mode at a scan rate of 8100 m/z s^{-1} with an aimed ion charge control of 100 000 in a maximal fill time of 200 ms and a total of four scans were averaged to obtain a MS spectrum. The three most abundant peptides and preferentially doubly charged ions were selected on each MS spectrum for further isolation and fragmentation. The MS/MS scanning was performed in the ultrascan resolution mode at a scan rate of 26 000 m/z s^{-1} with an aimed ion charge control of 300 000 and a total of six scans were averaged to obtain an MS/MS spectrum. The complete system was fully controlled by ChemStation Rev. B.01.03 (Agilent Technologies) and EsquireControl 6.1 Build 78 (Bruker Daltonics) softwares. Mass data collected during LC-MS/MS analyses were processed using the software tool DataAnalysis 3.4 Build 169 and converted into .mgf files. The MS/MS data were analysed using the MASCOT 2.2.0. algorithm (Matrix Science, London, UK) to search against an in-house generated protein database composed of protein sequences of Viridiplantae down-loaded from http://www.ncbi.nlm.nih.gov/sites/entrez (on 6 March 2008) concatenated with reversed copies of all sequences (2× 478 588 entries). Spectra were searched with a mass tolerance of 0.5 Da for MS and MS/MS data, allowing a maximum of 1 missed cleavage by trypsin and with carbamidomethylation of cysteines, oxidation of methionines, and N-terminal acetylation of proteins speci-fied as variable modifications. Protein identifications were validated when at least two peptides with high quality MS/MS spectra (Mascot ion score greater than 31) were detected. In the case of one-peptide hits, the score of the unique peptide must be greater (minimal 'difference score' of 6) than the 95% significance Mascot threshold (Mascot ion score >51). For the estimation of the false positive rate in protein identification, a target-decoy database search was performed (Elias and Gygi, 2007).

GC-MS-based metabolite profiling

For GC-MS analysis, polar metabolite fractions were extracted from 60 mg ±10 % (FW) frozen plant material, ground to a fine powder, with methanol/chloroform. The fraction of polar metabolites was prepared by liquid partitioning into water/methanol (polar fraction) and chlo-roform (non-polar fraction) as described earlier (Roessner *et al.*, 2000; Wagner *et al.*, 2003). Metabolite samples were derivatized by methoxyamination, using a 20 mg ml^{-1} solution of methoxyamine hydrochloride in pyridine, and subsequent trimethylsilylation, with *N*-methyl-*N*-

(trimethylsilyl)-trifluoroacetamide (Fiehn *et al.*, 2000; Roessner *et al.*, 2000). A C_{12}, C_{15}, C_{19}, C_{22}, C_{28}, C_{32}, and C_{36} n-alkane mixture was used for the determination of retention time indices (Wagner *et al.*, 2003). Ribitol and deuterated alanine were added for internal standardization. Samples were analysed using GC-TOF-MS (ChromaTOF software, Pegasus driver 1.61; LECO, http://www.leco.com). Four sample types (±Mn and ±Si), each with five replicates, comprised an experimental data set of 20 chromatograms. The chromatograms and mass spectra were evaluated using the TagFinder software (Luedemann *et al.*, 2008).

Sample preparation for the metabolite profiling of the AWF was adapted to the respective volumes and metabolite concentrations. In this case 200 μl of AWF_{H_2O} and AWF_{NaCl} were extracted to obtain a polar metabolite fraction, without further addition of water. The volume of methanol/chloroform was reduced to 50% as were the reagents for methoxyamination and silylation. Four sample types (two Mn treatments, and two Si treatments), each with four to five replications, in total 35 chromatograms, were analysed as described above.

In parallel free phenols (in the following termed non-polar apoplastic fraction) were extracted from AWF_{H_2O} and AWF_{NaCl}. First AWF was alkalized with 0.5 N NaOH (ratio 1:1) overnight. Afterwards samples were acidified by adding 5 N HCl (ratio 0.1125:1). Phenols were then extracted by shaking with diethylether (ratio 1:1). Samples were then dried under nitrogen atmosphere and prepared for GC-MS analysis as described for AWF. Four sample types (two Mn treatments and two Si treatments), each with five to six replications, resulted in 48 chromatograms, which were processed as described.

GC-MS metabolite profiles were processed after conversion into NetCdf file format using the TagFinder (Luedemann *et al.*, 2008) and NIST05 software (http://www.nist.gov/srd/mslist.htm). The mass spectral and retention index (RI) collection of the Golm metabolome database (Kopka *et al.*, 2005; Schauer *et al.*, 2005) was used for manually supervised metabolite identifcation. Yet non-identified metabolic components were disregarded for the present study. Peak height representing a mass specific arbitrary detector response was used for screening the relative changes of metabolite pools. The initial mass specific responses were normalized by leaf fresh weight and ribitol recovery. AWF metabolite profiles were normalized to ribitol recovery and AWF total volume of partitioned polar (water/methanol) and non-polar (chloroform) AWF fractions.

Statistical analysis of GC-MS profiles

Prior to statistical data assessment, response ratios were calculated based on the mean response of each metabolic feature from all samples of an experimental data set. Response ratios were subsequently $\log_{10}$-transformed. Independent component analysis (ICA) and missing value substitution was as described earlier (Scholz *et al.*, 2005). ICA was carried out using the first five principal compo-

nents obtained from a set of manually identified metabolites represented by at least three specific mass fragments each. Basic calculations of relative changes in abundance of specific metabolites due to Mn and Si treatment were made with the Microsoft Excel 2000 software program and respective embedded algorithms. For pairwise comparisons thresholds of 2-fold change in pool size and $P < 0.05$ (*t* test,) were applied or levels of significance indicated, namely ***, **, and * representing $P < 0.001$, 0.01, and 0.05, respectively. Logarithmic transformation of response ratios approximated the required Gaussian normal distribution of metabolite profiling data (Schaarschmidt *et al.*, 2007).

Statistical analysis of Mn and Si concentrations and apoplastic enzyme activities

Statistical analysis, if not mentioned otherwise, was carried out using SAS Release v8.0 (SAS Institute, Cary, NC). Results from analysis of variance are given according to their level of significance as ***, **, and * for $P < 0.001$, 0.01, and 0.05, respectively. Pairwise comparisons were by using Student's *t* test.

Results

Exposing the plants to 50 μM Mn supply rapidly increased the Mn tissue concentration in the second oldest trifoliate leaf over the 4 d treatment period (Fig. 1A). This led to typical Mn toxicity symptoms (brown spots) after 2 d increasing up to 70 spots cm^{-2} after 4 d of Mn treatment (Fig. 1B). Silicon supply did not affect leaf Mn accumulation (Fig. 1A). However, in contrast to plants cultivated without Si, Si-treated plants developed only slight Mn toxicity symptoms (2–5 spots cm^{-2}) after 4 d of Mn treatment (Fig. 1B).

Since our previous work indicated a particular role of the apoplast in the expression of Mn toxicity and Mn tolerance in cowpea, our studies were focused on the AWF in particular. In this study, the leaves were submitted to a fractionated AWF extraction procedure yielding a free water-soluble fraction (AWF_{H_2O}) and an ionically bound NaCl-extractable (AWF_{NaCl}) fraction. The Mn concentration in the AWF_{H_2O} increased rapidly after 1 d of toxic Mn supply and then it tended to decrease again (Fig. 2A). Silicon application consistently enhanced the monomeric Si concentration in the AWF_{H_2O} (Fig. 2B) compared with non Si-treated plants, without consistently affecting the apoplastic Mn concentration (Fig. 2A). In the AWF_{NaCl}, the Mn concentration of the second trifoliate leaf steeply increased after 1 d Mn treatment and remained stable at a higher level than in the AWF_{H_2O} (Fig. 2C). In Si-treated plants, the Mn concentrations were slightly higher. Silicon treatment enhanced the monomeric Si concentration (Fig. 2D), but with Mn treatment duration this difference disappeared.
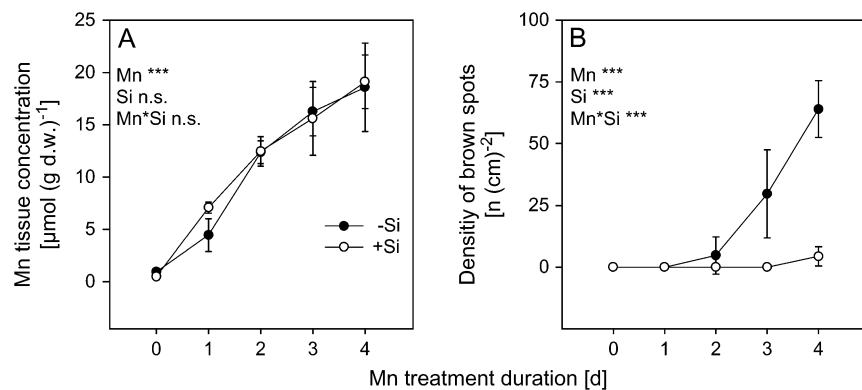
Fig. 1. Effect of Mn treatment duration and Si supply on (A) the Mn tissue concentration and (B) the density of brown spots of the second oldest trifoliate leaves of the Mn-sensitive cowpea cultivar TVu 91. After 2 weeks of preculture at 0.2 µM Mn the Mn supply was increased to 50 µM for 4 d. Silicon was supplied throughout plant culture. Results of the analysis of variance are given according to their level of significance as ***, **or * for $P < 0.001$, 0.01, 0.05, respectively. Values are means ±SD with $n=16$.
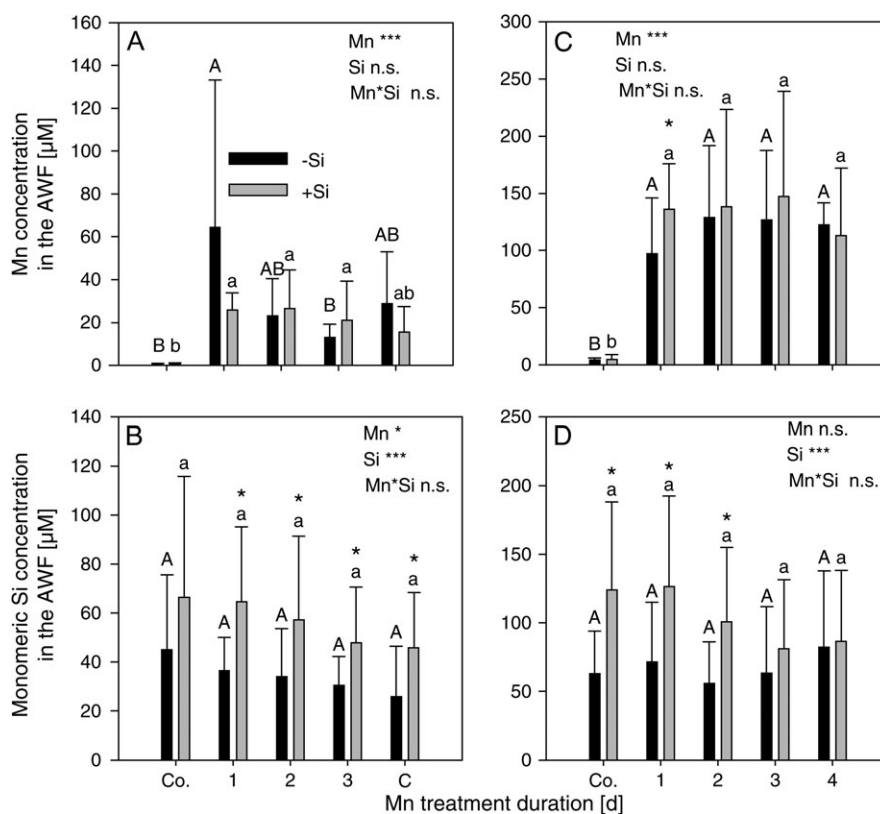
Fig. 2. Effect of Mn treatment duration and Si supply on the Mn concentration (A, C) and the monomeric Si concentration (B, D) in the water-soluble apoplastic fraction (A, B), and in the ionically bound apoplastic fraction (C, D) of the second oldest trifoliate leaves of the Mn-sensitive cowpea cultivar TVu 91. After 2 weeks of preculture at 0.2 µM Mn, the Mn supply was increased to 50 µM for 4 d. Silicon was supplied throughout plant culture. Results of the analysis of variance are given according to their level of significance as ***, **or * for $P < 0.001$, 0.01, or 0.05, respectively. Upper case and lower case letters indicate significant differences between Mn treatment duration of –Si and +Si-treated plants, respectively, at $P < 0.05$. An asterisk on top of the columns indicates siginificant differences between the Si treatments for at least $P < 0.05$ according to Tukey. Values are means ±SD with $n=16$.

In order to demonstrate the capability of the POD isoenzymes to catalyse both H_2O_2-producing and -consuming POD activities, AWF_{NaCl} was separated by BN-PAGE and PODs in-gel stained first for NADH-*per*oxidase followed by staining for guaiacol-peroxidase activity (Fig. 3A, B). Despite the quite low NADH-*per*oxidase activity stain-ing intensity the gels revealed that each isoenzyme showed both activities. Staining with guaiacol visualized major isoenzymes more clearly: one isoenzyme smaller than P1 and four isoenzymes greater than P1, all with low activity levels (Fig. 3B). After 6 d of Mn treatment, three additional guaiacol-peroxidase bands appeared greater than the P6

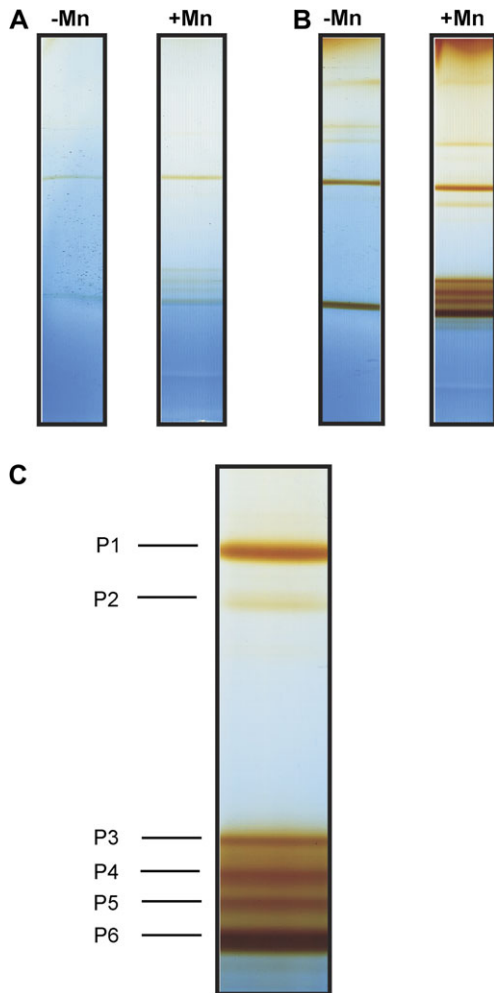**Fig. 3.** AWF$_{NaCl}$-proteins of the second oldest trifoliate leaf of the Mn-sensitive cultivar TVu 91 stained for (A) NADH-*per*oxidase and (B) guaiacol-peroxidase activity after separation by BN-PAGE. After preculture with 0.2 µM Mn (–Mn) for 14 d, plants received 50 µM (+Mn) Mn for 6 d. Fifty µl of concentrated AWF$_{NaCl}$ containing ionically bound proteins (–Mn 60 µg, +Mn 112 µg) were loaded onto the gels. Proteins were NBT-stained for NADH-*per*oxidase (A) at pH 5.0 with 16 mM MnCl$_2$, 1.66 mM *p*-coumaric acid, 0.625 mg ml^{-1} NBT, and 0.22 mM NADH. For guaiacol-peroxidase, proteins were stained (B) in 18 mM guaiacol (in 9 mM Na$_2$HPO$_4$) and 0.03% H$_2$O$_2$ at pH 6.0. Close up (C) shows marked isoenzymes (P1, P3, P5, P6) that were chosen for elution and further characterzation of pH optima and substrate specificity.

isoenzyme and one with a MW smaller than P1. One isoenzyme with a MW greater than P1 disappeared owing to elevated Mn supply. An extensive study of in-gel activity-stained BN gels loaded rigourously with the same protein quantities comparing Mn treatments with and without Si supply and differentiating between AWF$_{H_2O}$ and AWF$_{NaCl}$ proteins revealed that all isoenzymes were qualitatively present in both Mn treatments, but elevated Mn supply led to an increased abundance of isoenzymes P3 and P5, especially in the water-soluble fractions (see Supplementary Figs S1 and S2 at *JXB* online). In Mn-control plants Si-treatment did not affect the POD isoenzyme pattern. Silicon

delayed but not suppressed the Mn-mediated increase in the number of POD isoenzymes in the AWF$_{H_2O}$ (see Supplementary Fig. S1 at *JXB* online).

Figure 3C shows a close-up of those POD isoenzymes (clearly appearing after 4 d of Mn treatment), which were chosen for further characterization after elution of the proteins from the gels: P1, P3, P5, and P6, whereas P2 and P4 were only sequenced. The eluted isoenzymes P3, P5, and P6, showed both NADH-*per*oxidase and guaiacol-peroxidase activities (Fig. 4A, B). The specific activity was highest for P6 followed by P5. The POD isoenzyme P1 had very little guaiacol-peroxidase activity. The pH optimum for all isoenzymes showing activity was consistently 6.5 for guaiacol-peroxidase activity (Fig. 4A) and pH 5.5 for NADH-*per*oxidase activity (Fig. 4B).

All marked POD activity-stained protein bands (Fig. 3) were cut; proteins were digested and analysed by liquid chromatography-coupled mass spectrometry (LC-MS/MS). MS/MS searches did not always lead to a positive identification in cowpea (*Vigna unguiculata*) since its genome has not yet been sequenced, but can lead to the identification of peptides in related sequences of green plants (Viridiplantae) downloaded from http://www.ncbi.nlm.nih.gov/sites/entrez. Forty-four unique proteins were identified in the green plants database. To estimate the false positive rate of identification, a target-decoy database was performed (Elias and Gygi, 2007), and no additional protein was identified in reversed sequences, suggesting that our dataset contained very few or no false-positive identifications. A list of all resulting peptides, as well as their identities, is given as supplementary data (see Supplementary Table S2 at *JXB* online). Among these peptides, 11 peptides belonging to class III peroxidases could be identified (Fig. 5). At least three overlapping peptides provide evidence for at least three distinct gene products. Three peptides with amino acid substitutions were exclusively found in POD isoenzyme P1 when extracted with NaCl from Mn-treated plants (Figs 3, 5; see SupplementaryTable S2 at *JXB* online).

Since apoplastic NADH-*per*oxidase proved to react most sensitively to toxic Mn supply and this enzyme has been attributed a key role in the expression of Mn toxicity (Fecht-Christoffers *et al.*, 2006, 2007), the NADH-*per*oxidase activity of the isoenzymes was further characterized for interaction with different commercially available phenols (Fig. 6) at the optimum pH identified above with *p*-coumaric acid and Mn as a cofactors. Among the 10 phenols tested, *p*-coumaric acid and vanillic acid proved to be the most effective cofactors for all isoenzymes particularly at the highest concentration level. Benzoic acid showed only little activity at the higher concentrations even though the response pattern was similar, whereas ferulic acid activated NADH-*per*oxidase activity only at a lower concentration. All other phenols did not induce NADH-*per*oxidase activity. As shown above (Fig. 4A, B) the isoenzyme P6 showed by far the highest activity.

The potential inhibitory effect of phenols on NADH-*per*oxidase activity was studied by adding eight phenols to the reaction mixture and monitoring their effect on
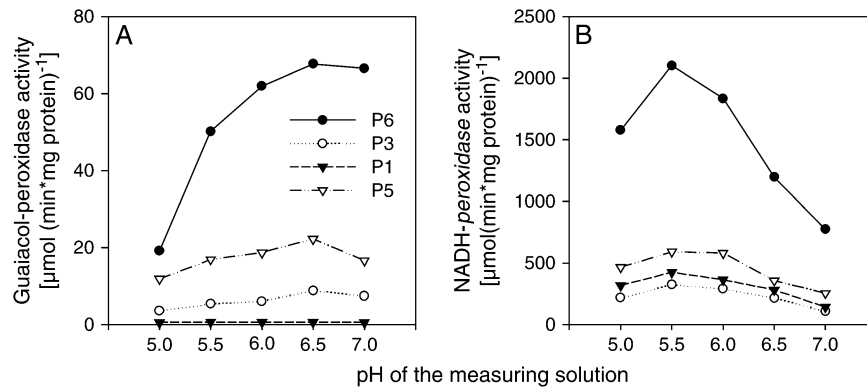
Fig. 4. Determination of the pH optimum of (A) the guaiacol-peroxidase activity and of (B) the NADH-*per*oxidase activity of four POD isoenzymes of the Mn-sensitive cowpea cultivar TVu 91. POD isoenzymes were eluted from BN gels that separated a mixture of AWF_{H_2O} and AWF_{NaCl} extracted from the second oldest trifoliate leaf of Mn-treated (4 d) and ±Si-treated (as described in the Materials and methods) plants. Measurements were done in succinate buffer with pH values between 5.0 and 7.0 using 0.5 steps between the pH values. Measuring solution (0.1 M succinate buffer) for the determination of NADH-*per*oxidase activity consisted of 16 mM $MnCl_2$, 1.66 mM *p*-coumaric acid, and 0.22 mM NADH, measuring solution for guaiacol-peroxidase activity consisted of 18 mM guaiacol (in 90 mM succinate buffer) and 0.03% H_2O_2.

p-coumaric acid-stimulated enzyme activity (Fig. 7). Benzoic acid and vanillic acid did not reduce the *p*-coumaric acid-stimulated NADH-*per*oxidase activity and even enhanced it. All other phenols inhibited NADH-*per*oxidase activity by about 50% (ferulic and syringic acid) and by >90% for the other phenols. This was true for all isoenzymes.

Since metabolites were shown to affect apoplastic PODs strongly (see above and Fecht-Christoffers *et al.*, 2006), the bulk-leaf metabolome was studied in a broad range approach using GC-MS and independent component analyses (ICA) (Scholz *et al.*, 2004). Applying ICA, sample clusters were investigated according to the major variances due to the treatment-induced qualitative and quantitative changes of metabolite pools. This variance criterion was augmented by subsequent pairwise or multiple probability-based statistical significance testing.

In our factorial experimental designs both Mn and Si treatment proved to be among the most important independent components (Fig. 8A) of our data sets resulting from the bulk-leaf tissue. The analysis revealed that Mn (IC01) and Si (IC04) treatments induced significant changes in the metabolome. Silicon treatment clearly induced significant conditional differences among the Mn control treatment but only slight differences in Mn-treated plants. The Mn effect was mainly caused by changes in the concentrations of amino acids (serine, threonine, asparagine, aspartic acid), phenyl-alcohols (coniferylalcohol), organic acids (gluconic acid), and sugar alcohols (sorbitol) as revealed by ICA loadings. The Si effect was mainly due to differences in sugars (galactose) and organic acids (gluconic acid).

In view of the particular role of the activity of apoplastic peroxidases in Mn toxicity additionally the AWF_{H_2O} and the AWF_{NaCl} were subjected to a metabolomic analysis. The ICA showed clear differences between the AWF fractions (IC01, Fig. 8B). Also, manganese treatment induced separate clustering in both AWF fractions (IC02). In this

approach Si did not affect the sample clustering according to treatment-mediated metabolite differences. As revealed by ICA loadings, metabolites mainly responsible for the differential clustering of AWF_{H_2O} and AWF_{NaCl} were GABA, organic acids (malic acid, ribonic acid, gluconic acid), amino acids (threonine), and sugars (xylose, erythrose, fucose) among many currently unidentified metabolites. The clustering according to the Mn treatment was mainly caused by organic acids (maleic acid, malic acid, nicotinic acid, itaconic acid), amino acids (threonine, alanine), sugars (xylose, fructose, tagatose), and phenols (3-hydroxybenzoic acid).

Further fractionation of the leaf apoplastic metabolome by an extraction method specifically yielding non-polar metabolites revealed a clustering of samples according to the infiltration solution, confirming the strong experimental impact of the AWF fraction on the result (Fig. 8C). Loadings derived from ICA showed that among other currently unknown metabolites, mainly organic acids (fumaric acid, malic acid, succinic acid, citric acid, 3-oxoglutaric acid) and phenylpropanoids (*cis*- and *trans*-cinnamic acid, *p*-hydroxybenzoic acid) were responsible for this clustering.

Quantification of relative changes between treatments yielded five different phenols in this non-polar extract (Table 1) among them ferulic acid, *p*-hydroxybenzoic acid, and *p*-coumaric acid which had shown considerable inhibiting or enhancing effects, respectively, on *in vitro* NADH-*per*oxidase activity. Ferulic acid and *p*-coumaric acid were analytically separated into respective *cis*- and *trans*-isomers, whereas in the *in vitro* NADH-*per*oxidase activity-enhancing/inhibiting tests (Figs 6, 7) commercially available isomer mixtures were used. Both ferulic acid isomers showed a significant 2–4-fold reduction in abundance in Mn-treated plants compared with control plants in the AWF_{H_2O} fraction. A comparison of ±Si treatments revealed a significantly increased abundance of benzoic acid and of ferulic
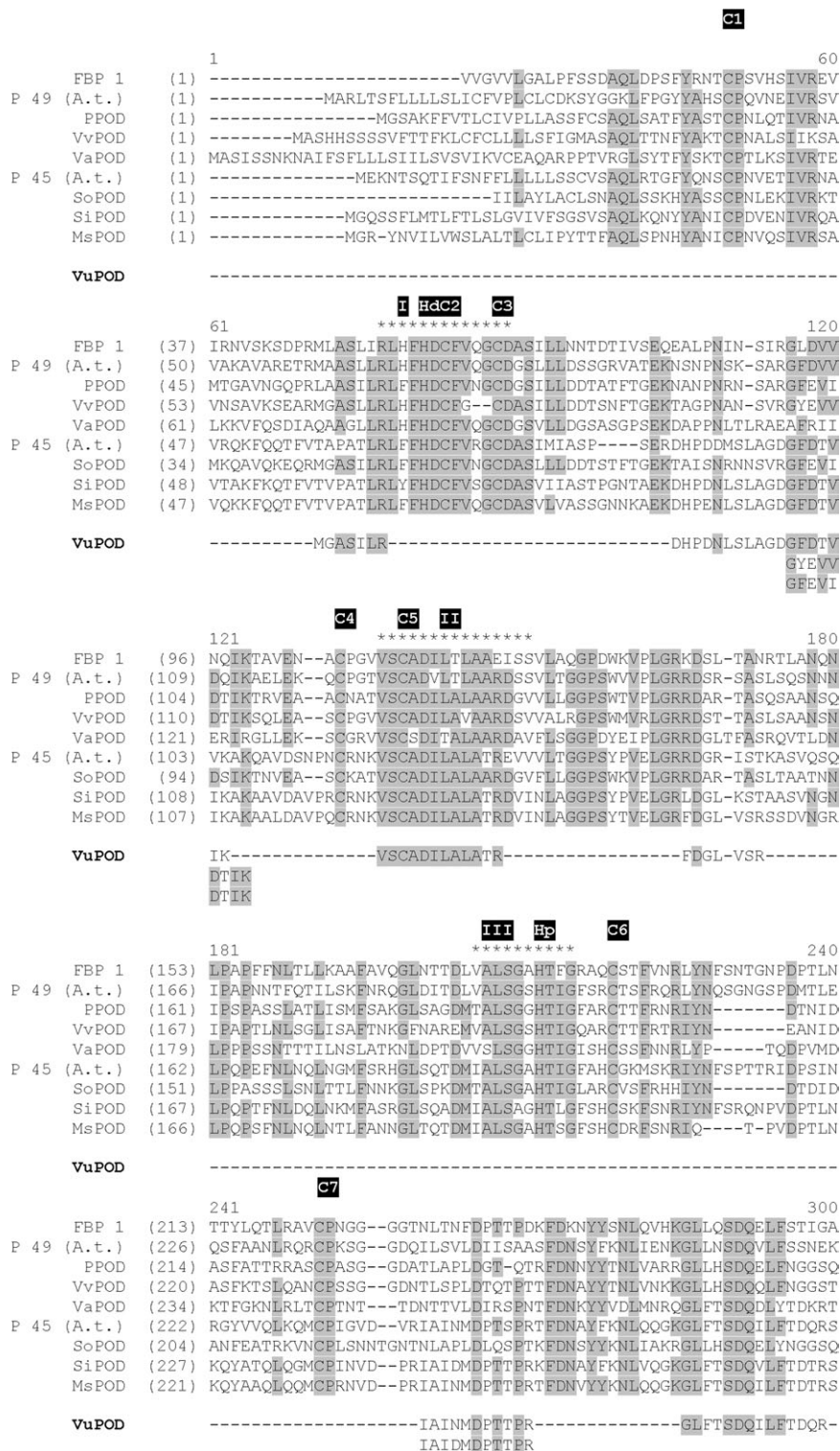
Fig. 5. Alignment of determined and deduced amino acid (aa) sequences of peroxidases of various plant species and all 11 nano LC-MS/MS-identified peroxidase peptide sequences from cowpea. Amino acid positions conserved in at least 50% of the sequences are underlaid in grey. Asterisks (*) indicate the conserved distal haem-binding domain (I), the central conserved domain of unknown function (II), and the proximal haem-binding domain. The eight cysteines (C1–C8) and the distal (Hd) and proximal (Hp) histidines are indicated, too. Abbreviations: FBP1, French Bean Peroxidase 1 (acc no. AF149277); P49 (A.t.), POD isoenzyme 49 from *Arabidopsis thaliana* (acc. no. O23237); PPOD from *Populus* ssp. (acc. no. AAX53172); VvPOD from *Vitis vinfera* (acc. no. CAO48839); VaPOD from *Vigna angularis* (acc. no. BAA01950); P45 (A.t.) POD isoenzyme 45 from *Arabidopsis thaliana* (acc. no. Q96522); SoPOD from *Spinacia oleracea* (acc. no. CAA71493); SiPOD from *Sesamum indicum* (acc. no. ABB89209), MsPOD from *Medicago sativa* (acc. no. CAC38106); VuPOD, POD peptide sequences of *Vigna unguiculata* (this study).

```
                                                                    C8
              301                                                          360
    FBP 1   (271) DTIDIVNRFSSNQTLFFESFKAAMIKMGNIGVLTGSQGEIRKQCNFVNGNSAGLATLATK
  P 49 (A.t.) (284) S-RELVKKYAEDQGEFFEQFAESMIKMGNISPLTGSSGEIRKNCRKINS-----------
    PPOD    (271) --DALVRTYSTNGATFARDFAAAMVRMGNISPLTGTNGEIRRNCRVVN-----------
    VvPOD   (278) --DAVVNTYSTRSTTFFTDFANAMVRMGNLSPLTGTSGQIRTNCRKTN-----------
    VaPOD   (291) --RGIVTSFAVNQSLFFEKFVFAMLKMGQLSVLTGNQGEIRANCSVRNANSKAFLSSVVE
  P 45 (A.t.) (280) --RSTVNSFANSEGAFRQAFITAITKLGRVGVLTGNAGEIRRDCSRVN-----------
    SoPOD   (264) --DALVTRYSKSNAAFAKDFVAAIIKMGNISPLTGSSGEIRKNCRFIN-----------
    SiPOD   (285) --RNTVNTWASNPQAFNAAFIQAITKLGRVGVKTARNGNIRFDCGRFN-----------
    MsPOD   (279) --RNTVNSFATNGNVFNANFITAMTKLGRIGVKTARNGKIRTDCTVL-----------

    VuPOD         ------------------------MGNISPLTGSSGEIR-------------------
                                          MGNISPLTGTNGEIR


              361      371
    FBP 1   (331) ESSEDGLVSSI
  P 49 (A.t.) (332) -----------
    PPOD    (317) -----------
    VvPOD   (324) -----------
    VaPOD   (349) NVAQEFIEM--
  P 45 (A.t.) (326) -----------
    SoPOD   (310) -----------
    SiPOD   (331) -----------
    MsPOD   (324) -----------

    VuPOD         -----------
```

Fig. 5. (*continued*)

acid isomers (more than 3-fold) in Si-treated plants only in the AWF_{NaCl} fraction. In Si-treated plants, high Mn supply led to increased concentrations of benzoic acid in the AWF_{H_2O} fraction and to decreased abundance of ferulic acid compared with plants grown at low Mn supply. A comparison of +Mn/+Si with +Mn/–Si (Mn toxicity-showing) plants showed significantly decreased *p*-hydroxybenzoic acid concentrations. A major, however not significant, increase in abundance 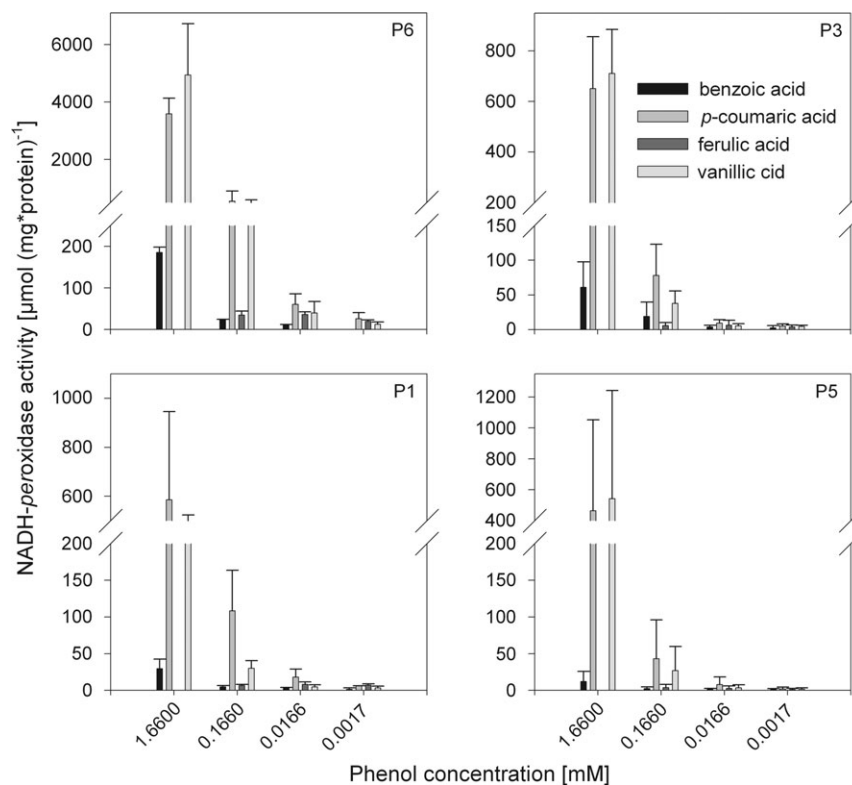of *cis*-ferulic acid is indicated in the +Mn/+Si plants not showing Mn toxicity symptoms. NADH-*per*oxidase activity enhancing *p*-coumaric acid showed no changes in abundance in each of the comparisons.

A three-factorial ANOVA showed benzoic acid, *p*-hydroxybenzoic acid, and ferulic acid to be significantly affected by Mn (Table 2). Silicon treatment significantly affected *p*-hydroxybenzoic acid and *cis*-ferulic acid. Highly significant differences between the apoplastic fractions were found for all identified phenylpropanoids except ferulic acid and benzoic acid. Also, the infiltration solution had a clear impact on *p*-hydroxybenzoic acid, *p*-coumaric acid, and *trans*-sinapic acid. None of the two or three way interactions were significant (not presented).

Discussion

Effect of Mn and Si on apoplastic Mn fractions

Manganese is readily taken up by plants independent of the Si supply, but the expression of toxicity symptoms was suppressed by Si treatment (Fig. 1A, B) which is in line with results previously published for cowpea (Horst *et al.*, 1999; Iwasaki *et al.*, 2002a, b). This Si-enhanced Mn tolerance has been explained entirely in cucumber (Rogalla and Römheld, 2002) or partly in cowpea (Iwasaki *et al.*, 2002a, b) by a reduction of the free Mn in the apoplast through enhanced strong binding of Mn by the cell walls in Si-treated plants. However, in the present study neither the AWF_{H_2O} (Fig. 2A)

nor the 5-fold higher AWF_{NaCl} (Fig. 2C) Mn concentrations differed clearly owing to Si treatment. This might be explained by different growing conditions of the plants and Mn extraction procedures. Nevertheless, this clearly shows that, in cowpea, the expression of Mn toxicity cannot be explained just on the basis of the free and exchangeable Mn concentration in the leaf apoplast, in agreement with the conclusion drawn by Iwasaki *et al.* (2002a, b). They postulated a particular role of the monomeric Si in enhancing Mn tolerance. Indeed, also in our study the monomeric Si concentration was consistently higher in Si-treated plants in the AWF_{H_2O} (Fig. 2B) and initially also in the AWF_{NaCl} (Fig. 2D) fraction. The decreasing concentration of monomeric Si with increasing Mn treatment duration in the latter fraction possibly due to polymerization and/or strong binding in the cell walls (incrustation) may explain why Si treatment did not prevent but only delayed the formation of brown spots (Fig. 1B) with extended Mn treatment duration.

Manganese and Si-induced changes of peroxidase activities

All isoenzymes were shown to perform both reaction cycles (Figs 3, 4). Mn treatment led to an increased abundance of POD isoenzymes (Fig. 3; see Supplementary Fig. S1 at *JXB* online; Fecht-Christoffers *et al.*, 2003b) thus explaining enhanced apoplastic POD activities (Fecht-Christoffers *et al.*, 2006). Silicon treatment only delayed but not suppressed the Mn-mediated increased abundance of POD isoenzymes (see Supplementary Fig. S1 at *JXB* online), which is in line with the delayed but not prevented development of Mn toxicity symptoms (Fig. 1B). Using higher protein loadings BN-PAGE separation of AWF_{H_2O} and AWF_{NaCl} protein did not reveal qualitative but only quantitative differences in POD isoenzyme patterning between the infiltration solutions, indicating that all detected isoforms are principally water-soluble (see

Fig. 6. Effect of different phenols on NADH-*per*oxidase activity of four POD isoenzymes. POD isoenzymes were eluted from BN-gels (see Fig. 4 and Materials and methods). Measuring solution (0.1 M succinate buffer, pH 5.5) consisted of 16 mM $MnCl_2$, 0.22 mM NADH, and phenols (benzoic acid, *p*-coumaric acid, ferulic acid, caffeic acid, chlorogenic acid, gallic acid, protocatechuic acid, syringic acid, and vanillic acid) in different concentrations (1.6 mM, 0.166 mM, 0.016 mM, and 0.0016 mM). Only the four displayed phenols induced NADH-*per*oxidase activity. For the calculation of enzyme activities, extinction coefficients were adapted (see Supplementary Table S1 at *JXB* online). Results are from two independent experiments including plant growth and protein separation.

Supplementary Fig. S2 at *JXB* online), even though a low protein loading could lead to the opposite conclusion (Fig. 3; see Supplementary Fig. S1 at *JXB* online). The results confirm a particular role of PODs in the AWF_{H_2O} in the modulation of Mn toxicity (Fecht-Christoffers *et al.*, 2006, 2007).

Characterization of the identified peroxidases

The sequencing of the POD activity-showing 1D-BN protein bands P1 to P6 revealed that each band was composed of more than one protein (see Supplementary Table S2 at *JXB* online) confirming BN/SDS-PAGE results previously published by Fecht-Christoffers *et al.* (2003*b*). All bands led to the identification of at least one peptide with high sequence homology to peroxidases in the NCBI green plants database. In total, 11 different peptides have been identified belonging to the class III secretory peroxidase family including sequences for the conserved so-called 'domain II' (Hiraga *et al.*, 2001)/'domain D' (Delannoy *et al.*, 2003) (Fig. 5, see Supplementary Table S2 at *JXB* online). Three overlapping peptide sequences provide evidence for the presence of at least three distinct genes encoding for class III secretory peroxidases (Fig. 5). Three peptides with amino acid substitutions (including the overlapping peptide

sequences: Fig. 5) were exclusively found in AWF_{NaCl}-extracted isoenzyme P1 from Mn-treated plants (Figs 3, 5; see Supplementary Table S2 at *JXB* online) indicating specific apoplastic binding properties.

As MS analyses did not result in complete POD sequences, one can only speculate about the total number of distinct class III secretory peroxidases in *Vigna unguiculata*. Based on *in gel* activity stainings, peroxidases of a wide range of MW were detected (Fig. 3; see Supplementary Figs S1 and S2 at *JXB* online). There are several possibilities leading to such great differences in the MW of the isoenzymes. (i) Class III peroxidases belong to a large multigenic family even though they are distinct proteins (Passardi *et al.*, 2004) with MWs ranging 28 kDa up to 60 kDa (Hiraga *et al.*, 2001). (ii) A protein oligomer showing peroxidase activity is conceivable, such as a peroxidase dimer. (iii) Depending on the degree of *N*-glycolization, the native MW may vary thus leading to changes in the MW in the order of P3–P6 (Fig. 3). (iv) Other apoplastic proteins than class III peroxidases might also have peroxidative activity, i.e. oxidoreductase and/or auxin-binding (germin-like) proteins, even though the sequencing results did not identify proteins that could perform a peroxidative reaction (see Supplementary Table S2 at *JXB* online).

The role of pH in controlling apoplastic POD isoenzyme activities

A pH optimum seems to be necessary for POD self-protection (Olsen *et al.*, 2003). In addition, the pH could be an important regulatory factor for the relative performance of either the peroxidative or the peroxidative–oxidative reaction cycle of the enzyme. If an apoplastic pH of about 5.0–6.0 as shown for *Vicia faba* (Mühling and Läuchli, 2000) is assumed, both POD cycles are expected to have high activities within this range (Fig. 5), indicating that the apoplastic pH is not decisive in regulating the relative contribution of each reaction cycle in response to toxic Mn supply. The determined pH optimum for both POD activities is precisely in the range of the recommended pH of the measuring solutions for POD activity determination *in vitro* in studies investigating lignin formation (Kärkönen *et al.*, 2002). However, in studies on the hypersensitive stress response to leaf pathogens, NADH-*per*oxidase-mediated H_2O_2 production proved to be related to an alkalization of the apoplast (Bolwell *et al.*, 1995, 1998, 2001; Pignocchi and Foyer, 2003) suggesting differences between biotic and abiotic stress responses.
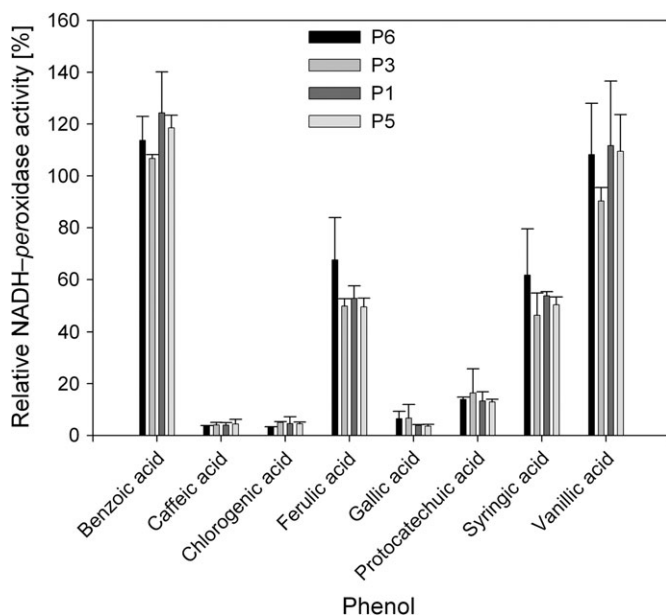
Fig. 7. Effect of combining different phenols with *p*-coumaric acid as the control phenol on the induction capability for NADH-*per*oxidase activity of four POD isoenzymes. POD isoenzymes were eluted from BN gels (see Fig. 3 and Materials and methods). Measuring solution (0.1 M succinate buffer, pH 5.5) consisted of 0.166 mM *p*-coumaric acid, 16 mM $MnCl_2$, 0.22 mM NADH, and 0.0166 mM of one of the following phenols to examine interactions between phenols: benzoic acid, ferulic acid, caffeic acid, chlorogenic acid, gallic acid, protocatechuic acid, syringic acid, or vanillic acid. Activities are expressed as relative values in relation to activities when *p*-coumaric acid was applied alone (in the same concentration). For the calculation of enzyme activities, extinction coefficients were adapted (see Supplementary Table S1 at *JXB* online). Results are from two independent experiments including plant growth and protein separation.
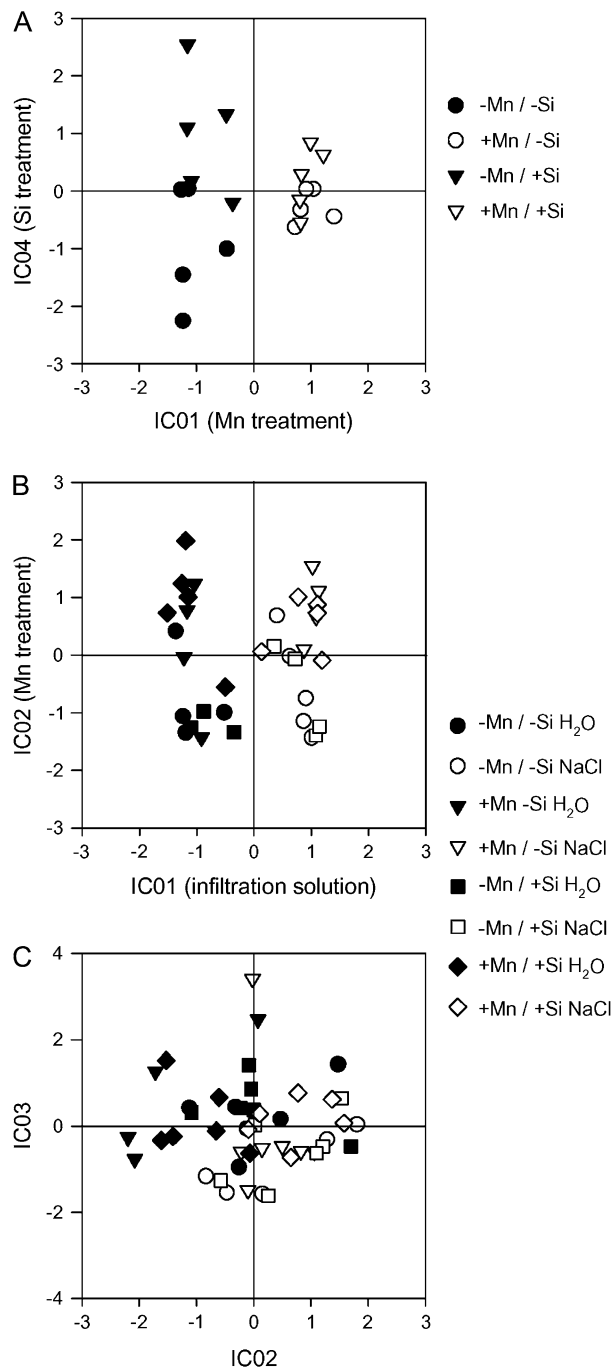

Fig. 8. ICA plot of the GC-MS-accessible (A) bulk-leaf metabolome, (B) the polar AWF metabolites, and (C) the non-polar metabolites extracted from the AWF. The second oldest trifoliate leaf of the Mn-sensitive cultivar TVu 91 was tested for Mn and Si effects. After 14 d of preculture with or without Si, plants received 50 µM Mn (+Mn) for 3 d or 0.2 µM Mn (–Mn) continuously. Bulk-leaf, AWF- and non-polar apoplastic metabolites were extracted (*n*=5 and 6, respectively) as described in the Materials and methods. ICA was conducted using MetaGeneAlyse at http://metagenealyse.mpimp-golm.mpg.de.

Table 1. Identified phenols (GC-MS) in the non-polar fraction of the leaf AWF recovered after infiltration with H_2O or NaCl

Displayed are the relative pool-size changes of each phenol calculated on the basis of response ratios. The effects of these phenols on the NADH-peroxidase activity (see Figs 6 and 7) of apoplastic peroxidase isoenzymes are also shown. After 14 d of preculture, ±Si-treated plants of the Mn-sensitive cowpea cv. TVu91 received 50 μM Mn for 3 d or 0.2 μM Mn continuously. Statistical testing of changes in metabolite abundance were calculated using $\log_{10}$-transformed response ratios. An asterisk denotes significant differences at least at $P < 0.05$ ($n=6$), respectively (t test).

Detected metabolites NADH-	+Mn/–Mn		+Si/–Si		+Mn+Si/–Mn+Si		+Mn+Si/+Mn–Si		Effect of phenol on peroxidase activity[a]
	AWF_{H_2O}	AWF_{NaCl}	AWF_{H_2O}	AWF_{NaCl}	AWF	AWF_{NaCl}	AWF_{H_2O}	AWF_{NaCl}	
Benzoic acid	1.41[c]	1.35	0.91	1.32*	1.49*	1.14	0.97	1.12	weak induction/no inhibition
p-Hydroxybenzoic acid[b]	1.47	1.61	0.87	0.65	1.03	1.23	0.61*	0.50*	No induction/50% inhibition
cis-p-Coumaric acid	1.00	0.81	0.95	1.13	1.06	0.62	1.00	0.86	Strong induction
cis-Ferulic acid	0.24*	0.30*	1.03	3.77*	0.70	0.35*	2.96	4.37	Weak induction/50% inhibition
trans-p-Coumaric acid	0.88	0.82	0.84	0.95	0.97	0.59	0.92	0.68	Strong induction
trans-Ferulic acid	0.44*	2.31	1.34	3.61*	0.50	0.37*	1.52	0.57	Weak induction/50% inhibition
trans-Sinapic acid	2.39	0.81	n.d.[+]	0.72	n.d.[++]	0.90	n.d.[++]	0.80	Not examined

[a] from Figs. 6 and 7.
[b] After identification of p-hydroxybenzoic acid, this phenol was additionally tested with respect to NADH-peroxidase activity. In addition to the 50% inhibitory effect it showed no induction capability for NADH-peroxidase activity for each isoenzyme tested.
[c] Numbers are calculated ratios of the response ratios (not $\log_{10}$-transformed) within the individual comparison. ANOVA did not reveal a significant Mn×Si interaction.
[+],[++] were not detected (n.d.) in +Si and +Mn+Si treatments, respectively.

Table 2. Identified phenols (GC-MS) in the non-polar fraction of the leaf AWF recovered after infiltration with H_2O or NaCl (Inf.).

Displayed are the p-values derived from analysis of variance based on $\log_{10}$-transformed response ratios ($n=6$). For the effects of these phenols on the NADH-peroxidase activity of apoplastic peroxidase isoenzymes see Figs 6 and 7 as well as Table 1. After 14 d of preculture, ±Si-treated plants of the Mn-sensitive cowpea cultivar TVu 91 received 50 μM Mn for 3 d or 0.2 μM Mn continuously.

Metabolite	Mn	Si	Inf.
Benzoic acid	0.0032	0.2786	0.2615
4-Hydroxybenzoic acid[a]	0.0093	<0.0001	<0.0001
cis-4-Hydroxycinnamic acid	0.4236	0.5636	<0.0001
cis-Ferulic acid	<0.0001	0.0012	0.4433
trans-4-Hydroxycinnamic acid	0.1269	0.1057	<0.0001
trans-Ferulic acid	0.0129	0.2470	0.3870
trans-Sinapic acid	0.4671	0.1685	0.0039

[a] After identification of p-hydroxybenzoic acid, this phenol was additionally tested with respect to NADH-peroxidase activity. In addition to the 50% inhibitory effect, it showed no induction capability for NADH-peroxidase activity for each isoenzyme tested.

The role of metabolites in controlling apoplastic POD isoenzyme activities: metabolite profiling

In a broad range metabolomic approach, it has been shown that Mn toxicity induced changes in the bulk-leaf metabolome according to ICA (Fig. 8A; IC01) consistent with our recent results showing that Mn toxicity also affects symplastic reactions using a combined proteomic/transcriptomic and physiological approach (Führs *et al.*, 2008). The involvement of the symplast in Mn toxicity is in line with studies using other plant species showing Mn toxicity-induced reduced CO_2 assimilation capacity (González and Lynch, 1997, 1999; González *et al.*, 1998, common bean;

Nable *et al.*, 1988; Houtz *et al.*, 1988, tobacco) accompanied by reduced chlorophyll contents (Gonzalez and Lynch, 1999; Gonzalez *et al.*, 1998, common bean; Moroni *et al*, 1991, wheat), and high Mn-accumulation rates in chloroplasts (Lidon *et al.*, 2004, rice). Our metabolomic approach also showed that Si supply led to a particular clustering of the total leaf metabolome as revealed by ICA (Fig. 8A; IC04). This is in agreement with the work of Maksimović *et al.* (2007) on Si/Mn-toxicity interaction in cucumber who concluded that Si supply modulates the phenol metabolism.

A closer investigation of the apoplastic metabolome using AWF_{NaCl} and AWF_{H_2O} revealed that the infiltration solution (IC01; Fig. 8B) was the most important factor explaining differences between the extracted metabolome fractions. Manganese (IC02) but not Si treatment affected both AWF metabolome fractions. The ICA loadings identified organic acids, amino acids, and sugars to be responsible for Mn and infiltration solution-related clusterings (Fig. 8B), whereas phenolic compounds were unexpectedly low since Fecht-Christoffers *et al.* (2006, 2007) reported a Mn-induced change in the apoplastic water-soluble phenol composition (and at later toxicity stages even in phenol concentration) using HPLC separation of leaf AWF_{H_2O} in cowpea (see discussion below). However, GC-MS based metabolite profiling typically covers mostly primary metabolites explaining the relative low abundance of phenolic compounds.

To overcome this problem, an additional special AWF-extraction procedure was applied yielding non-polar metabolites. This resulted in clustering only according to the infiltration solution (Fig. 8C; IC02, see discussion below). ICA loadings revealed, in addition to organic acids, that phenylpropanoids were mainly responsible for the clustering. Among other detected aromatic compounds, ferulic acid was identified as a clearly Mn and Si-affected phenol (Tables 1, 2; see discussion below).

Overall, the broad-range metabolite profiling in the bulk-leaf extract (Fig. 8A, ICA01) and the AWF (Fig. 8B; ICA02) revealed a clear difference related to the Mn treatment. The Si effect was less clearly expressed. A preliminary metabolite-specific evaluation of the metabolites indicates alterations of metabolic pathways mainly related to organic acids, amino acids, and sugars/sugar alcohols. A detailed evaluation and discussion of the qualitative changes in polar apoplastic metabolites is beyond the scope of this paper and will be subject of a subsequent paper.

The role of phenols in controlling apoplastic NADH-peroxidase activity

Analysing the AWF_{H_2O} using HPLC, Fecht-Christoffers *et al.* (2006) separated water-soluble phenols in the apoplast. A Mn treatment not only increased the peak size but also led to at least two additional peaks, which supported their conclusion that the presence of phenols in the apoplast is decisive for the expression of Mn toxicity/Mn tolerance in cowpea leaf tissue. However, they failed to identify the phenols. Our gas chromatography–mass spectrometry approach allowed us to identify five phenols. However, the method does not allow absolute concentrations to be determined but only relative treatment-related concentration changes. Also, it was not possible to identify most phenols directly in the AWF. Therefore, the aqueous AWF was extracted with diethylether which led to a concentration of the phenols but at the same time only yielded non-polar metabolites. Thus, the applied technique did not allow us to identify and quantify all the phenols present in the apoplast which is a major focus of ongoing research. Nevertheless, among the phenols identified (Tables 1, 2), four were found which had been tested for their effect on NADH-peroxidase activity *in vitro*. Only *p*-coumaric acid had a strong activity-enhancing effect. Ferulic acid and *p*-hydroxybenzoic acid had only a weak or lacking stimulating effect, but a strong inhibiting effect when combined with *p*-coumaric acid. Benzoic acid only weakly enhanced and did not inhibit NADH-peroxidase activity (Figs 6, 7; Table 1).

The three-factorial analysis of variance of the treatment-induced changes in the abundance of the phenols (Table 2) revealed that Mn treatment significantly affected the concentrations of benzoic, *p*-hydroxybenzoic and, most clearly, ferulic acid, whereas Si treatment affected *p*-hydroxybenzoic and again most clearly *cis*-ferulic acid. Looking at the comparison of means of the treatment-specific relative pool-size changes of the individual phenols (Table 1), it appears that the change in the concentration in the apoplast of ferulic acid particularly plays a key role in the expression of Mn toxicity symptoms: a reduction of the concentration leading to a reduced inhibition of NADH-peroxidase activity is characteristic for leaves showing Mn toxicity symptoms (+Mn/–SI), while Mn-tolerant leaf tissue (–Mn/+Si; +Mn/+Si) is characterized by an enhanced accumulation. The constitutive effect of Si on an enhanced abundance of ferulic acid seems to be stong enough to counteract the Mn-induced

reducing effect (compare +Mn +Si/–Mn +Si, Table 1). Also, it appears that Si affects the phenol concentration more in the AWF_{NaCl} (as indicated by the high infiltration solution effect on the phenols in Table 2) than in the AWF_{H_2O} corroborating results demonstrating Si-mediated changes of apoplastic Mn-binding properties (Iwasaki *et al.*, 2002a; Rogalla and Römheld, 2002). However, ferulic acid and benzoic acid, in particular, were not affected by the infiltration solution, indicating specific apoplastic binding properties in the apoplast for each phenol regardless of Si nutrition (Table 1). The Si-induced significantly higher abundance of benzoic acid might be of minor importance, given the rather weak NADH-peroxidase activity-enhancing effect (Fig. 8). However, the lowered concentration of NADH-peroxidase activity-inhibiting *p*-hydroxybenzoic acid in the presence of Si at high Mn supply is not in line with the above expressed line of thinking. Thus it appears a more detailed and quantitative investigation of the phenols present in the leaf apoplast is necessary to understand Mn toxicity and Mn tolerance fully.

In conclusion, the results presented here confirm the hypothesized role of apoplastic NADH-peroxidase and its activity-modulating phenols in Mn toxicity and Si-enhanced Mn tolerance. Isoenzyme BN gel-profiling of POD enzymes and their characterization after elution from the gels, and metabolite profiling of the bulk-leaf and the AWF appear to be powerful tools in enhancing the physiological and molecular understanding of Mn toxicity and Mn tolerance.

Supplementary data

Supplementary data can be found at *JXB* online.

Supplementary Fig. S1. 1D BN-PAGE resolution of AWF_{H_2O} and AWF_{NaCl} proteins (16 μg) after 0 and 4 d of Mn treatment of ±Si-treated plants of the Mn-sensitive cowpea cultivar TVu 91.

Supplementary Fig. S2. 1D BN-PAGE resolution of AWF_{H_2O} and AWF_{NaCl} proteins (180 μg) after 0 d and 4 d of Mn treatment of the Mn-sensitive cowpea cultivar TVu 91.

Supplementary Table S1. Extinction coefficients for the calculation of NADH-peroxidase activities of different POD isoenzymes supplied with different phenols in changing concentrations as shown in Figs 4, 6, and 7.

Supplementary Table S2. Peptide sequences of apoplastic leaf proteins sequenced with LC-MS/MS.

Acknowledgements

References

Bolwell GP, Butt VS, Davies DR, Zimmerlin A. 1995. The origin of the oxidative burst in plants. *Free Radical Research* **23,** 517–532.

Bolwell GP, Davies DR, Gerrish C, Auh C-K, Murphy TM. 1998. Comparative biochemistry of the Oxidative Burst prodiced by rose and French Bean cells reveals two distinct mechanisms. *Plant Physiology* **116,** 1379–1385.

Bolwell GP, Page A, Piślewska M, Wojtaszek P. 2001. Pathogenic infection and the oxidative defences in plant apoplast. *Protoplasma* **217,** 20–32.

Bradford MM. 1976. A rapid and sensitive method for the quantitation of microgram quantities of protein utilizing the principle of protein–dye binding. *Analytical Biochemistry* **72,** 248–254.

Delannoy E, Jalloul A, Assigbetsé K, Marmey P, Geiger JP, Lherminier J, Daniel JF, Martinez C, Nicole M. 2003. Activity of class III peroxidases in the defense of cotton to bacterial blight. *Molecular Plant–Microbe Interactions* **16,** 1030–1038.

Elias JE, Gygi SP. 2007. Target-decoy search strategy for increased confidence in large-scale protein identifications by mass spectrometry. *Nature Methods* **4,** 207–214.

Epstein E. 1999. Silicon. *Annual Review of Plant Physiolgy and Plant Molecular Biology* **50,** 641–664.

Fecht-Christoffers MM, Braun H-P, Lemaitre-Guillier C, VanDorsselear A, Horst WJ. 2003*b*. Effect of Mn toxicity on the proteome of the leaf apoplast in cowpea. *Plant Physiology* **133,** 1935–1946.

Fecht-Christoffers MM, Führs H, Braun H-P, Horst WJ. 2006. The role of hydrogen peroxide-producing and hydrogen peroxide-consuming peroxidases in the leaf apoplast of cowpea in manganese tolerance. *Plant Physiology* **140,** 1451–1463.

Fecht-Christoffers MM, Maier P, Horst WJ. 2003*a*. Apoplastic peroxidase and ascorbate are involved in manganese toxicity and tolerance of *Vigna unguiculata*. *Physiologia Plantarum* **117,** 237–244.

Fecht-Christoffers MM, Maier P, Iwasaki K, Braun H-P, Horst WJ. 2007. The role of the leaf apoplast in manganese toxicity and tolerance in cowpea (*Vigna unguiculata* L. Walp). In: Sattelmacher B, Horst WJ, eds. *The apoplast of higher plants: compartment of storage, transport, and reactions*. Dordrecht, The Netherlands: Springer, 307–322.

Fiehn O, Kopka J, Trethewey RN, Willmitzer L. 2000. Identification of uncommon plant metabolites based on calculation of elemental compositions using gas chromatography and quadrupole mass spectrometry. *Analytical Chemistry* **72,** 3573–3580.

Führs H, Hartwig M, Molina LEB, Heintz D, Van Dorsselaer A, Braun H-P, Horst WJ. 2008. Early manganese-toxicity response in *Vigna unguiculata* L.: a proteomic and transcriptomic study. *Proteomics* **8,** 149–159.

González A, Lynch JP. 1997. Effects of manganese toxicity on leaf CO_2 assimilation of contrating common bean genotypes. *Physiologia Plantarum* **101,** 872–880.

González A, Lynch JP. 1999. Subcellular and tissue Mn compartmentation in bean leaves under Mn toxicity stress. *Australian Journal of Plant Physiology* **26,** 811–822.

González A, Steffen KL, Lynch JP. 1998. Light and excess manganese: Implications for oxidative stress in common bean. *Plant Physiology* **118,** 493–504.

Halliwell B. 1978. Lignin synthesis: the generation of hydrogen peroxide and superoxide by horseradish peroxidase and its stimulation by manganese (II) and phenols. *Planta* **140,** 81–88.

Hiraga S, Sasaki K, Ito H, Ohashi Y, Matsui H. 2001. A large family of class III plant peroxidases. *Plant and Cell Physiology* **42,** 462–468.

Horst WJ. 1980. Genotypische Unterschiede in der Mangan-Toleranz von Cowpea (*Vigna unguiculata*). *Angewandte Botanik* **54,** 377–392.

Horst WJ. 1982. Quick screening of cowpea genotypes for manganese tolerance during vegetative and reproductive growth. *Zeitschrift für Pflanzenernährung und Bodenkunde* **145,** 423–425.

Horst WJ. 1983. Factors responsible for genotypic manganese tolerance in cowpea (*Vigna unguiculata*). *Plant and Soil* **72,** 213–218.

Horst WJ. 1988. The physiology of Mn toxicity. In: Webb MJ, Nable RO, Graham RD, Hannam RJ, eds. *Manganese in soil and plants*. Dodrecht/Boston/London: Kluwer Academic Publishers, 175–188.

Horst WJ, Fecht M, Naumann A, Wissemeier AH, Maier P. 1999. Physiology of manganese toxicity and tolerance in *Vigna unguiculata* (L.) Walp. *Journal of Plant Nutrition and Soil Science* **162,** 263–274.

Horst WJ, Marschner H. 1978*a*. Effect of silicon on manganese tolerance of bean plants (*Phaseolus vulgaris* L.). *Plant and Soil* **50,** 287–303.

Horst WJ, Marschner H. 1978*b*. Symptome von Manganüberschuss bei Bohnen (*Phaseolus vulgaris*). *Zeitschrift für Pflanzenernährung und Bodenkunde* **141,** 129–142.

Houtz RL, Nable RO, Cheniae GM. 1988. Evidence for effects on the *in vivo* activity of ribulose-bisphosphate carboxylase/oxygenase during development of Mn toxicity in tobacco. *Plant Physiology* **86,** 1143–1149.

Iwasaki K, Maier P, Fecht M, Horst WJ. 2002*a*. Effects of silicon supply on apoplastic manganese concentrations in leaves and their relation to manganese tolerance in cowpea (*Vigna unguiculata* (L.) Walp.). *Plant and Soil* **238,** 281–288.

Iwasaki K, Maier P, Fecht M, Horst WJ. 2002*b*. Leaf apoplastic silicon enhances manganese tolerance of cowpea (*Vigna unguiculata*). *Journal of Plant Physiology* **159,** 167–173.

Iwasaki K, Matsumura A. 1999. Effect of silicon on alleviation of manganese toxicity in pumpkin (*Cucurbita moschata* Duch cv. Shintosa). *Soil Science and Plant Nutrition* **45,** 909–920.

Jänsch L, Kruft V, Schmitz UK, Braun HP. 1996. New insights into the composition, molecular mass and stoichiometry of the protein complexes of plant mitochondria. *The Plant Journal* **9,** 357–368.

Kärkönen A, Koutaniemi S, Mustonen M, Syrjänen K, Brunow G, Kilpeläinen I, Teeri TH, Simola LK. 2002. Lignification related enzymes in *Picea abies* suspension cultures. *Physiologia Plantarum* **114,** 343–353.

Kopka J, Schauer N, Krueger S, *et al*. 2005. GMD@CSB.DB: the Golm metabolome database. *Bioinformatics* **21,** 1635–1638.

Lidon FC, Barreiro MG, Ramalho JC. 2004. Manganese accumulation in rice: implications for photosynthetic functioning. *Journal of Plant Physiology* **161,** 1235–1244.

Luedemann A, Strassburg K, Erban A, Kopka J. 2008. TagFinder for the quantitative analysis of gas chromatography-mass spectrometry

(GC-MS) based metabolite profiling experiments. *Bioinformatics* **24,** 732–737.

Maksimović JD, Bogdanović J, Maksimović V, Nikolic M. 2007. Silicon modulates the metabolism and utilization of phenolic compounds in cucumber (*Cucumis sativus* L.) grown at excess manganese. *Journal of Plant Nutrition and Soil Science* **170,** 739–744.

Marschner H. 1995. *Mineral nutrition in higher plants*, 2nd edn. London, UK: Academic Press.

Moroni JS, Briggs KG, Taylor GJ. 1991. Chlorophyll content and leaf elongation rate in wheat seedlings as a measure of manganese tolerance. *Plant and Soil* **136,** 1–9.

Mühling KH, Läuchli A. 2000. Light-induced pH and K^+ changes in the apoplast of intact leaves. *Planta* **212,** 9–15.

Nable RO, Houtz RL, Cheniae GM. 1988. Early inhibition of photosynthesis during development of Mn toxicity in tobacco. *Plant Physiology* **86,** 1136–1142.

Olsen LF, Hauser MJB, Kummer U. 2003. Mechanism of protection of peroxidase activity by oscillatory dynamics. *European Journal of Biochemistry* **270,** 2796–2804.

Passardi F, Cosio C, Penel C, Dunand C. 2005. Peroxidases have more functions than a Swiss army knife. *Plant Cell Reports* **24,** 255–265.

Passardi F, Longet D, Penel C, Dunand C. 2004. The class III peroxidase multigenic family in rice and its evolution in land plants. *Phytochemistry* **65,** 1879–1893.

Pignocchi C, Foyer CH. 2003. Apoplastic ascorbate metabolism and its role in the regulation of cell signalling. *Current Opinion in Plant Biology* **133,** 443–447.

Roessner U, Wagner C, Kopka J, Trethewey RN, Willmitzer L. 2000. Simultaneous analysis of metabolites in potato tuber by gas chromatography–mass spectrometry. *The Plant Journal* **23,** 131–142.

Rogalla H, Römheld V. 2002. Role of leaf apoplast in silicon-mediated manganese tolerance of *Cucumis sativus* L. *Plant, Cell and Environment* **25,** 549–555.

Schaarschmidt S, Kopka J, Ludwig-Müller J, Hause B. 2007. Regulation of arbuscular mycorrhization by apoplastic invertases: enhanced invertase activity in the leaf apoplast affects the symbiontic interaction. *The Plant Journal* **51,** 390–405.

Schauer N, Steinhauser D, Strelkov S, *et al*. 2005. GC-MS libraries for the rapid identification of metabolites in complex biological samples. *FEBS Letters* **579,** 1332–1337.

Scholz M, Gatzek S, Sterling A, Fiehn O, Selbig J. 2004. Metabolite fingerprinting: detecting biological features by independent component analysis. *Bioinformatics* **20,** 2447–2454.

Scholz M, Kaplan F, Guy CL, Kopka J, Selbig J. 2005. Non-linear PCA: a missing data approach. *Bioinformatics* **21,** 3887–3895.

Shi Q, Bao Z, Zhu Z, He Y, Qian Q, Yu J. 2005. Silicon-mediated alleviation of Mn toxicity in *Cucumis sativus* in relation to activities of superoxide dismutase and ascorbate peroxidase. *Phytochemistry* **66,** 1551–1559.

Wagner C, Sefkow M, Kopka J. 2003. Construction and application of a mass spectral and retention time index database generated from plant GC/EI-TOF-MS metabolite profiles. *Phytochemistry* **62,** 887–900.

Wehrhahn W, Braun HP. 2002. Biochemical dissection of the mitochondrial proteome from *Arabidopsis thaliana* by three-dimensional gel electrophoresis. *Electrophoresis* **23,** 640–646.

Wissemeier AH, Horst WJ. 1992. Effect of light intensity on manganese toxicity symptoms and callose formation in cowpea (*Vigna unguiculata* (L.) Walp.). *Plant and Soil* **143,** 299–309.

Yamazaki I, Piette LH. 1963. The mechanism of aerobic oxidase reaction catalysed by peroxidase. *Biochimica et Biophysica Acta* **77,** 47–64.